

Phase-dependent ionization of hydrogen by intense sub-cycle pulses

J. T. KARPEL*  AND D. D. YAVUZ

Department of Physics, 1150 University Avenue, University of Wisconsin at Madison, Madison, Wisconsin 53706, USA

*Corresponding author: karpel@wisc.edu

Received 26 March 2018; accepted 1 May 2018; posted 3 May 2018 (Doc. ID 330498); published 23 May 2018

We have performed simulations and analytic calculations that show strong carrier-envelope phase dependence in the ionization of hydrogen atoms using intense sub-cycle sub-femtosecond laser pulses. When the pulse width is comparable to the classical orbit time of the initial bound state, sine-like pulses can ionize more than cosine-like pulses that have the same fluence. This result is the opposite of what is expected from a tunneling-like model, where the ionization probability primarily depends on the peak amplitude of the electric field during the pulse. © 2018 Optical Society of America

OCIS codes: (020.2649) Strong field laser physics; (320.7120) Ultrafast phenomena.

<https://doi.org/10.1364/OL.43.002583>

Since the laser was invented in 1960, physicists have pushed the boundaries of ultrafast intense-field physics by producing ever shorter and more powerful laser pulses. Every time the boundary has been pushed back, exciting new physics is discovered. Solid-state femtosecond lasers based on Ti:sapphire or fiber laser technology are now routine laboratory tools, giving physicists insight into fast quantum processes [1]. The next frontier to explore is the precise control of electron motion using sub-femtosecond, sub-cycle laser pulses [2].

Our particular interest in this regime is how sub-cycle modification of the waveform produced by a given power spectrum affects the interaction with the target system. For example, high-harmonic generation (HHG) processes can depend on the carrier-envelope phase (CEP) of the driving field [3]. Kolesik and colleagues have studied history-dependent effects in ionization using sub-cycle pulse trains [4]. Nakajima and coworkers found phase-dependent effects in the multi-photon regime when using sub-cycle pulses [5], as well as unexpected ionization probabilities in few-cycle pulses [6]. We are also motivated by the experiments with Rydberg atoms that used picosecond-timescale optical pulses to demonstrate that ionization processes behaved very differently when the duration of the pulse was similar to the classical orbit time of the initial state [7,8]. Heuristics and intuition based on the carrier frequency or instantaneous intensity of the laser field tend to have difficulty describing these effects because of interference between many quantum states.

In this Letter, we explore an example of the physics that could be seen with a sub-femtosecond, sub-cycle pulse. We present a numerical study of ionization by an intense laser pulse with duration close to the classical orbit time of the ground state of the hydrogen atom, and develop an approximate description for the ionization process in this regime based on the strong field approximation (SFA). Surprisingly, we find that pulses with sine-like CEPs can have greater ionization probabilities than cosine-like pulses that have the same power spectrum. This result is the opposite of what is expected from an intuitive tunneling-like model, which would predict that pulses with the largest electric field amplitudes would ionize more than pulses with smaller amplitudes.

We perform our numerical TDSE simulations on a spherical-harmonic/radial mesh in the length gauge. We evolve the wavefunction in time using equations of motion derived from the Lagrangian density and a split-operator version of the interaction term [9]. We generate a numeric eigenstate basis by partially diagonalizing the field-free discrete Hamiltonian using sparse matrix techniques. This basis is used to determine the initial state and to calculate inner products with field-free eigenstates. Our boundary condition is a radial cosine mask [10].

We consider linearly polarized laser pulses in carrier-envelope form [11] with an additional window function:

$$\mathcal{E}(t) = W_\tau(t)[\mathcal{E}_0 F_\tau(t) \cos(\omega_c t + \varphi) + \mathcal{E}_c], \quad (1)$$

where \mathcal{E}_0 is an amplitude prefactor, F_τ is an envelope function, W_τ is a window function, ω_c is the carrier frequency, φ is the CEP, and \mathcal{E}_c is the DC correction field amplitude. We call the parameter τ the pulse width.

We describe $\varphi = 0$ pulses as “cosine-like” and $\varphi = \pi/2$ pulses as “sine-like” based on their behaviors near $t = 0$, which are similar to envelope-less cosine or sine waves, respectively. For the same power spectrum (and, therefore, the same fluence) a cosine-like pulse has a peak electric field approximately $\sqrt{2}$ times larger than the sine-like pulse. We choose to use a sinc-shaped envelope, $\text{sinc}(x) \equiv \sin(x)/x$, because its Fourier transform has constant power over its bandwidth, such as an ideal supercontinuum source. Specifically, we use $F_\tau(t) = \text{sinc}(\pi t/\tau)$. This envelope has zeros at $t = n\tau$, $n = \pm 1, \pm 2, \dots$, and τ is the inverse of the cyclic frequency bandwidth of the pulse. We set a small fixed minimum frequency for the spectrum so that the pulse shape is nearly constant as we change τ . For the pulses used

in this Letter, $\omega_{\min} = 2\pi \times 30$ THz (a wavelength of $\lambda \approx 10$ μm), so that $\omega_c = \omega_{\min} + \pi/\tau$. The window function cuts off the electric field with a logistic rise/decay:

$$W_\tau(t) = \frac{1}{1 + \exp(-(t + t_w)/t_d)} - \frac{1}{1 + \exp(-(t - t_w)/t_d)}. \quad (2)$$

Typical parameters are $t_w = 30\tau$ and $t_d = \tau/5$. The window decreases the numeric fluence of the pulses compared to the analytic value by at most a few tenths of a percent. It also introduces Gibbs ringing at the edges of the spectrum. To correct for the introduction of a zero-frequency electric field component that is caused by windowing when $\varphi \neq \pi/2$, we add a small constant electric field \mathcal{E}_c that shares the same window function as the pulse, with an amplitude numerically chosen so that $\int_{t_i}^{t_f} dt \mathcal{E}(t) = 0$. This correction also causes small changes in the low-frequency components of the electric field. Combined, these effects cause perturbations in the ionization probability (compared to a simulation with infinite time bounds and no window) on the level of $\sim 0.5\%$ (verified by simulations with longer time bounds, without DC correction, or with fluence correction), which is not significant for the following discussion.

Pulse width scans showing the initial state overlap after interacting with a laser pulse for various fluences, and CEPs are shown in Fig. 1. A heatmap of the ratio between the initial state overlap of sine-like and cosine-like pulses is shown in Fig. 2.

Note that because we keep the pulse's fluences fixed, their bandwidths become very broad (hundreds of electron volts), and their electric fields become very large (tens of atomic electric fields) at short pulse widths. We expect our simulations to be less accurate in this regime since we neglect relativistic effects and spatial variation of the electric field. As a conservative limit, we cut off the curves and heatmap when the peak electric field of the cosine-like pulse reaches three atomic electric fields. Also note the large perturbations to the otherwise smooth curves near $\tau \approx 400$ as. This seems to be caused by the first inclusion of 10.4 eV photons to the pulse's spectrum, which allow single-

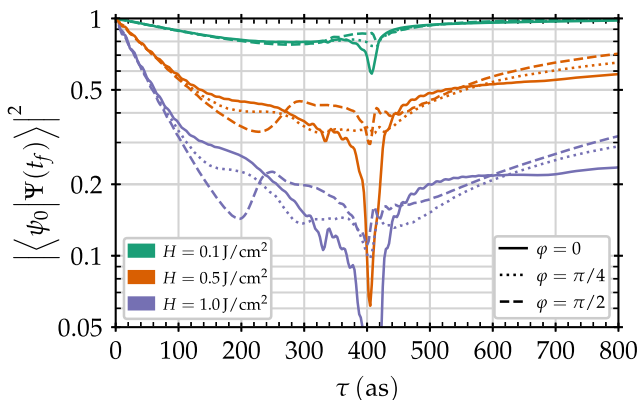


Fig. 1. Population remaining in the initial $1s$ state of hydrogen after interacting with a laser pulse as the pulse width τ is varied. For each fluence H , we perform numerical TDSE calculations for three values of the CEP φ . As the pulse width becomes comparable to the classical orbital period of the initial hydrogen ground state ($T_{cl} \approx 150$ as), the sine-like pulse ($\varphi = \pi/2$) ionizes much more than the cosine-like pulse ($\varphi = 0$), even though its peak electric field amplitude is lower by a factor of approximately $\sqrt{2}$.

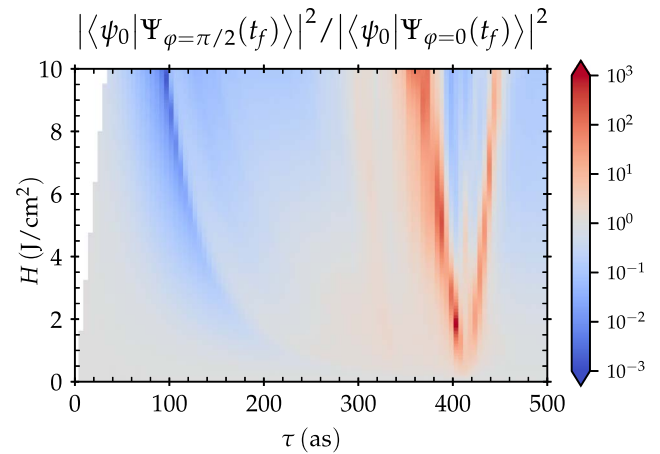


Fig. 2. Population remaining in the initial $1s$ state of hydrogen post-interaction for cosine-like ($\varphi = 0$) and sine-like ($\varphi = \pi/2$) pulses, calculated using the TDSE over a range of fluences H and pulse widths τ . Blue (red) coloration means that the sine-like pulse ionized more (less) than the cosine-like pulse. The white region is a result of cutting off the heatmap when the pulse's peak electric field amplitude reaches three atomic electric fields. The fractional difference in the remaining population can be very large (several orders of magnitude), despite the two pulses having the same fluence and pulse width.

photon transitions from the $1s$ ground state to the excited bound state $2p$. Unlike the rest of the scan, the simulations near this pulse width are quite sensitive to the perturbations of the pulse spectrum caused by windowing. We do not attempt to describe the behavior near $\tau \approx 400$ as in the following discussion.

As mentioned above, in this Letter, we are primarily concerned with the strong CEP dependence of the ionization probability at short pulse widths, comparable to the classical orbit time of the hydrogen ground state ($T_{cl} \approx 150$ as). The fact that such a dependence exists is not inherently surprising. For example, at longer pulse widths ($\tau \approx 1$ fs), cosine-like pulses ionize more than sine-like pulses. This is what we should expect from electric field amplitudes below the barrier-suppression regime: the dominant ionization mechanism is tunneling and, therefore, the dominant dependence of the ionization is on the maximum electric field amplitude [11]. Since the maximum electric field amplitude is larger for a cosine-like pulse than a sine-like pulse, the cosine-like pulse ionizes more. However, at pulse widths comparable to the classical orbit time, we see exactly the opposite behavior over a continuous range of pulse widths and fluences: sine-like pulses consistently ionize more than cosine-like pulses. Our intuition about how an instantaneous field amplitude relates to final ionization probability is not correct when the pulse is extremely short and has very high amplitude (large enough to be in the barrier-suppression regime, instead of the tunneling regime).

To investigate why the CEP dependence at short pulse widths develops and, in particular, why the sine-like pulses ionize more than the cosine-like pulses, despite having lower amplitudes, we have developed a simple description of the non-linear strong field interaction at these timescales. We begin with an expansion often used to analyze HHG using the SFA [12]. Our approach is similar to the techniques that lead to continuum state probability amplitudes that include rescattered

electrons [13] but, instead, we focus on calculating the bound state population directly.

Consider a system with a single bound state produced by a field-free Hamiltonian \hat{H}_0 that interacts with a linearly polarized external electric field $\mathcal{E}(t)$, calculated in the length gauge, $\hat{H}_I = -q\mathcal{E}(t)\hat{z}$. We expand the wavefunction as

$$|\Psi(t)\rangle = c_b(t)|b\rangle + \int_0^\infty dk \sum_{\ell, |m| \leq \ell} c_{k\ell m}(t)|k\ell m\rangle, \quad (3)$$

where $|b\rangle$ is the ket of the bound state, $|k\ell m\rangle$ is the ket of a delta-normalized (in wavenumber) continuum state labeled by the free-space wavenumber k and angular momentum quantum numbers ℓ and m , and $c_b(t)$ and $c_{k\ell m}(t)$ are the probability amplitudes for the bound and continuum states, respectively. In a typical ATI/HHG calculation, our goal would be to calculate $c_{k\ell m}(t)$ and determine the photoelectron spectrum [12]. Instead, we will calculate $c_b(t)$ to directly determine the ionization rate.

If we plug Eq. (3) into the TDSE, take the inner product with $\langle b|$ or $\langle k\ell m|$, and make the SFA, we get a set of coupled ordinary differential equations (written without explicit time dependences here for compactness):

$$\dot{c}_b = -i\omega_b c_b + i\frac{q}{\hbar}\mathcal{E} \sum_{\ell, |m| \leq \ell} \int_0^\infty dk c_{k\ell m} \langle b|\hat{z}|k\ell m\rangle, \quad (4a)$$

$$\begin{aligned} \dot{c}_{k\ell m} = & -i\omega_{k\ell m} c_{k\ell m} + i\frac{q}{\hbar}\mathcal{E} c_b \langle k\ell m|\hat{z}|b\rangle \\ & + i\frac{q}{\hbar}\mathcal{E} \sum_{\ell', |m'| \leq \ell'} \int_0^\infty dk' c_{k'\ell' m'} \langle k\ell m|\hat{z}|k'\ell' m'\rangle, \end{aligned} \quad (4b)$$

where $\omega_b = E_b/\hbar$ and $\omega_{k\ell m} = E_{k\ell m}/\hbar$ are the angular frequencies of the bound and continuum states, respectively. The last term in Eq. (4b) is the direct continuum-continuum coupling. There has been much discussion of ways to treat this interaction due to its importance in HHG [14–16]. In this Letter, we will neglect it entirely and formally integrate Eq. (4b), yielding

$$c_{k\ell m}(t) = -i\frac{q}{\hbar} \langle k\ell m|\hat{z}|b\rangle \int_{t_i}^t dt' c_b(t') \mathcal{E}(t') e^{-i\omega_{k\ell m}(t-t')}, \quad (5)$$

where t_i is the initial time, $c_b(t_i) = 1$, and we take the limit $t_i \rightarrow -\infty$. Neglecting the continuum-continuum interaction seems to be a reasonable approximation for the ultra-short timescales we are considering (at least for investigating the source of the CEP dependence reversal, as we will see). Plugging Eq. (5) back into Eq. (4a) results in a single integro-differential equation (IDE):

$$\begin{aligned} \dot{b}(t) = & -\frac{q^2}{\hbar^2} \mathcal{E}(t) \int_{-\infty}^t dt' b(t') \mathcal{E}(t') K_b(t-t'), \\ K_b(t-t') = & \sum_{\ell, |m| \leq \ell} \int_0^\infty dk |\langle k\ell m|\hat{z}|b\rangle|^2 e^{-i(\omega_{k\ell m} - \omega_b)(t-t')}, \end{aligned} \quad (6)$$

where $b(t) = c_b(t) \exp(i\omega_b t)$ and $K_b(t-t')$ is the kernel function. We use this IDE to analyze the behavior of the hydrogen atom, keeping in mind that it only describes coherent transitions between a single bound state and the continuum states that it can directly transition to, and that it ignores tunneling-like effects.

To compare the IDE to the TDSE, we numerically integrate the IDE with an approximate kernel. The bound state is the analytic hydrogen ground state, but the continuum states

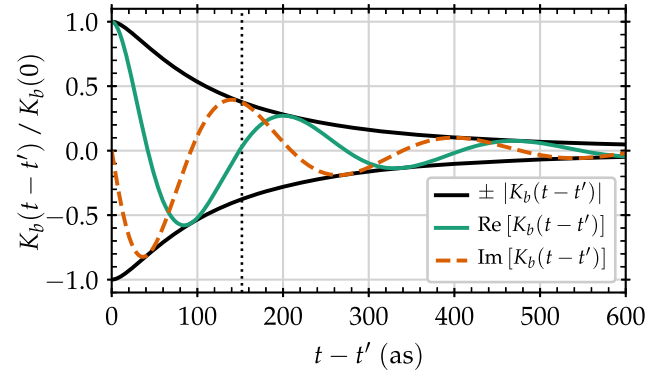


Fig. 3. Approximate kernel function $K_b(t-t')$ of the hydrogen ground state, calculated using delta-normalized spherical partial waves $\phi_{k\ell m}(r, \theta, \phi) \approx \sqrt{2/\pi} k j_\ell(kr) Y_\ell^m(\theta, \phi)$, where k is the free-space wavenumber, and j_ℓ is the spherical Bessel function with index ℓ , as the continuum states. The kernel has been normalized by $K_b(0) = a_0^2$, the Bohr radius squared. The timescale of the kernel is close to the classical orbit period of the ground state, $T_{cl} \approx 150$ as (vertical black dotted line).

are approximated by wavenumber-delta-normalized spherical partial waves, $\phi_{k\ell m}(r, \theta, \phi) \approx \sqrt{2/\pi} k j_\ell(kr) Y_\ell^m(\theta, \phi)$, where k is the free-space wavenumber, and j_ℓ is the spherical Bessel function with index ℓ . The resulting kernel, normalized by $K_b(0) = a_0^2$ (the Bohr radius squared), is shown in Fig. 3.

We numerically integrate the IDE using a fixed-time-step fourth-order Runge–Kutta algorithm (RK4) with $\Delta t \approx 1$ as. To check the accuracy of this method, we compared it to a general iterative algorithm for solving IDEs [17,18]. Both algorithms converged to the same results.

The pulse width and CEP scans calculated using the IDE are shown in Fig. 4, where they are compared to TDSE simulation scans. The IDE ionization probabilities do not have as much structure as those calculated using the TDSE and do not predict any significant ionization when the pulse amplitudes become small, as the pulse width increases at constant fluence. Nevertheless, the IDE scans display qualitatively similar features to the short-pulse-width regime of the TDSE scans: they predict that the ionization probability has a reversed CEP dependence when the pulse width becomes comparable to the classical orbit time. Since the IDE is modeling the second-order interaction between the bound state and the continuum states that it can transition to, we conclude that the primary driver of the CEP dependence in this regime is interference between the low- ℓ continuum electron wavefunction and the remaining bound state population, as described by $K_b(t-t')$.

An intuitive picture can be seen by approximating the IDE by restricting the integral in Eq. (6) to going back only by a time $\Delta \approx T_{cl}$ (on the basis that the kernel amplitude decreases exponentially as the time difference grows). We then approximate $b(t') \approx b(t)$, pull it out of the integral, and write

$$\begin{aligned} \dot{b}(t) \approx & -\frac{1}{\hbar^2} [q\mathcal{E}(t)] b(t) \int_{t-\Delta}^t dt' [q\mathcal{E}(t')] K_b(t-t'), \\ \dot{b}(t) \approx & -F(t) \tilde{v}(t, t-\Delta) b(t) / E_b, \end{aligned} \quad (7)$$

where $F(t)$ is the electric force on the electron, E_b is the Hartree energy, and $\tilde{v}(t, t-\Delta)$ is interpreted as the velocity of an electron in the laser field at time t after ionization at time

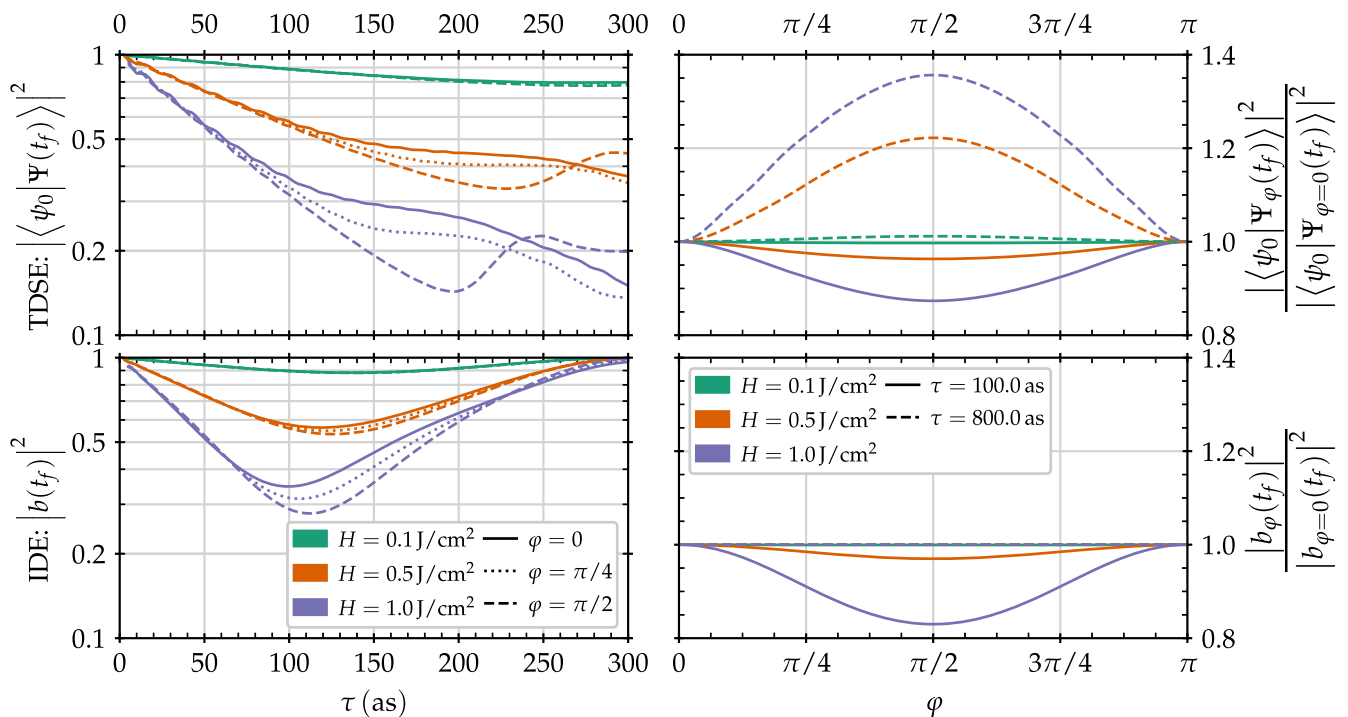


Fig. 4. Pulse width τ (left) and CEP φ (right) scans of the post-interaction initial state overlap, calculated using the TDSE (top) and the IDE (bottom). The CEP scans are normalized to the result of the $\varphi = 0$ pulse. The line colors correspond to fluences, and the line styles correspond to different CEPs on the left and different pulse widths on the right.

$t - \Delta$. This interpretation comes from the Lewenstein model of HHG, where the electron's action is integrated forward from the time of ionization to determine its dynamics [13]. The driving term can then be thought of as a quasi-classical quantity: the power (force multiplied by velocity) that the laser field is delivering to the electron compared to the binding energy.

A different way of approximating the IDE may be useful for longer pulses. For a femtosecond pulse, $\mathcal{E}(t')$ and $b(t')$ do not change significantly over the kernel timescale. We can pull them out of the integral in Eq. (6) and write

$$\dot{b}(t) \approx -\frac{q^2}{\hbar^2} \mathcal{E}^2(t) b(t) \int_0^\infty d\delta K_b(\delta), \quad (8)$$

where $\delta = t - t'$. The instantaneous ionization rate for a long pulse would then be proportional to $\mathcal{E}(t)^2$. Empirically-determined instantaneous ionization rates like this for femtosecond pulses with amplitudes in the barrier-suppression regime have been reported by other researchers [19,20]. We expect that including the continuum-continuum interaction in the IDE will give good agreement with these empirical rates, and we are interested in exploring this connection in future work.

Funding. National Science Foundation (NSF) (1306898); Wisconsin Alumni Research Foundation (WARF).

Acknowledgment. This Letter used the computing resources and assistance of the UW-Madison Center for High Throughput Computing. The authors thank Steve Harris and Alexei Sokolov for early discussions that led to this Letter, as well as Jeffrey Schmidt, Benjamin Lemberger, Zachary Buckholtz, and Francis Robicheaux for many helpful suggestions.

REFERENCES

1. T. W. Hänsch, *Rev. Mod. Phys.* **78**, 1297 (2006).
2. F. Krausz and M. Ivanov, *Rev. Mod. Phys.* **81**, 163 (2009).
3. D. Bauer, *Phys. Rev. Lett.* **94**, 057202 (2005).
4. M. Kolesik, J. M. Brown, J. V. Moloney, and D. Faccio, *Phys. Rev. A* **90**, 1 (2014).
5. T. Nakajima and S. Watanabe, *Opt. Lett.* **31**, 1920 (2006).
6. C. Liu and T. Nakajima, *Phys. Rev. A* **76**, 023416 (2007).
7. R. R. Jones, D. You, and P. H. Bucksbaum, *Phys. Rev. Lett.* **70**, 1236 (1993).
8. B. C. Yang and F. Robicheaux, *Phys. Rev. A* **91**, 043407 (2015).
9. K. J. Schafer, M. B. Gaarde, K. C. Kulander, B. Sheehy, and L. F. DiMauro, *AIP Conf. Proc.* **525**, 45 (2000).
10. J. L. Krause, K. J. Schafer, and K. C. Kulander, *Phys. Rev. A* **45**, 4998 (1992).
11. C. J. Joachain, N. J. Kylstra, and R. M. Potvliege, *Atoms in Intense Laser Fields* (Cambridge University, 2012).
12. M. Protopapas, C. H. Keitel, and P. L. Knight, *Rep. Prog. Phys.* **60**, 389 (1997).
13. W. Becker, F. Grasbon, R. Kopold, D. Milošević, G. Paulus, and H. Walther, *Advances in Atomic, Molecular, and Optical Physics*, B. Bederson and H. Walther, eds. (Academic, 2002), Vol. **48**, pp. 35–98.
14. M. Lewenstein, J. Mostowski, and M. Trippenbach, *J. Phys. B* **18**, L461 (1985).
15. J. G. Lewenstein, J. R. Kuklinski, and M. Lewenstein, *J. Phys. B* **19**, 3609 (1986).
16. N. Suárez, A. Chacón, M. F. Ciappina, J. Biegert, and M. Lewenstein, *Phys. Rev. A* **92**, 063421 (2015).
17. C. A. Gelmi and H. Jorquera, *Comput. Phys. Commun.* **185**, 392 (2014).
18. J. T. Karpel, *J. Open Source Softw.* **3**, 542 (2018).
19. D. Bauer and P. Mulser, *Phys. Rev. A* **59**, 569 (1999).
20. J. H. Bauer, *J. Phys. B* **49**, 145601 (2016).